Am J Cancer Res 2023;13(2):692-708
www.ajcr.us /ISSN:2156-6976/ajcr0144317

Brief Communication

Identification of necroptosis-related genes as prognostic indicators for lower-grade glioma

Xiaowan Huang[1], Somayeh Vafaei[2], Lingxia Li[1], Yunjiu Wang[1], Jian Sun[1], Yuzhen Gao[3], Jue Zhang[1]

[1]Department of Laboratory Medicine, Shuguang Hospital Affiliated to Shanghai University of Traditional Chinese Medicine, Shanghai 200021, China; [2]Department of Molecular Medicine, Faculty of Advanced Technologies in Medicine, Iran University of Medical Sciences, Tehran, Iran; [3]Department of Clinical Laboratory, Sir Run Run Shaw Hospital of Zhejiang University School of Medicine, Hangzhou 310016, Zhejiang, China

Received May 22, 2022; Accepted September 21, 2022; Epub February 15, 2023; Published February 28, 2023

Abstract: The purpose of this research is to develop a predictive model based on necroptosis-related genes to predict the prognosis and survival of lower grade gliomas (LGGs) efficiently. To achieve this goal, we searched for differentially expressed necrotizing apoptosis-related genes using the TCGA and CGGA databases. To construct a prognostic model, LASSO Cox and COX regression analyses were conducted on the differentially expressed genes. In this study, three genes were used to develop a prognostic model of necrotizing apoptosis, and all samples were split into high- and low-risk groups. We observed that patients with a high-risk score had a worse overall survival rate (OS) than those with a low-risk score. In the TCGA and CGGA cohorts, the nomogram plot showed a high capacity to predict overall survival of LGG patients. GSEA analysis revealed that the high-risk group was enriched for inflammatory responses, tumor-related pathways, and pathological processes. Additionally, the high-risk score was associated with invading immune cell expression. In conclusion, our predictive model based on necroptosis-related genes in LGG was shown to be effective in the diagnosis and could predict the prognosis of LGG. In addition, we identified possible targets related to necroptosis-related genes for glioma therapy in this study.

Keywords: Low-grade gliomas, necroptosis, TCGA, TMB, ssGSEA, prognosis

Introduction

Malignant gliomas of the central nervous system are typically aggressive and persistent [1]. Gliomas can be classified as either low-grade or high-grade according to criteria established by the World Health Organization (WHO) [2]. Despite the improved prognosis associated with low-grade gliomas (LGG), more than half of all LGG cases are deteriorated to high-grade gliomas after surgical resection and chemotherapy [3]. Even with vigorous combination treatment, LGGs have a dismal prognosis, particularly GBM, which has a median survival time (MST) of 14.6 months [4].

On the other hand, there is a better chance of survival from high-grade gliomas. Patients with the same grade of tumor can have drastically different survival rates and treatment responses due to the wide variety of gliomas [5]. Importantly, these widely used biomarkers cannot accurately predict the prognosis of glioma and cannot explain why patients with the same tumor grade have such varying outcomes [6]. Therefore, the discovery of significant and reliable glioma biomarkers is crucial for improving glioma diagnosis and therapy [7].

In comparison to autophagy, apoptosis, and pyroptosis, necroptosis stands out as a unique form of programmed cell death. In most cases, apoptosis is triggered by the activation of the proteins receptor interacting protein kinase 1 (RIPK1), RIPK3, and mixed lineage kinase domain-like (MLKL) [8]. Historically, necroptosis has been observed in patients with infections [9], liver impairment due to alcohol or drugs [10], and spinal cord injuries [11]. Besides, a growing body of research suggested that it could play multiple roles in the initiation and dissemination of cancer [12]. Necroptosis genes could present in nearly all malignancies and correlate with a poor outcome in cancer

patients [13]. Necroptosis is a part of the inflammatory necrosis process [14], and there is mounting evidence that it may aid in the metastasis and invasion of certain cancers [15]. However, necroptosis's mechanism and its ability to predict glioma outcome have not been widely explored.

Necroptosis may either hinder or encourage the growth of cancers, depending on the kind and stage of the tumors [16]; However, the link between necroptosis-related genes and LGGs remains uncertain. In this study, genes involved in necroptosis were examined in gliomas and healthy brain tissue samples from the TCGA, CGGA, and GTEx databases to establish a model for predicting the LGGs outcome. Besides, we used bioinformatics analysis to demonstrate a relationship between LGGs and necroptosis in our research.

Materials and method

Data collection and preprocessing

The Cancer Genome Atlas (TCGA, https://www.tcga.org/) and the China Glioma Genome Atlas Project (CGGA, http://www.cgga.org.cn/) databases were used to gather transcriptome profiles and clinical data for patients with LGGs (until November 2, 2021). The Genotype-Tissue Expression Project (GTEx, https://xenabrowser.net/) database contains the transcriptome profiles of 1152 normal brain tissues. The TCGA database was queried for 523 patients with low-grade gliomas [17]. As a validation set, 420 patients were gathered from the CGGA database.

Differentially expressed genes (DEGs) identification

All datasets have their expression data and standardized to fragment per kilobase million (FPKM) values. Differential genes were found using online bioinformatics tools (GEPIA2, http://gepia2.cancer-pku.cn); we defined statistically significant differential genes as those with |log2FC|>1, adjp0.05. A total of 59 necroptosis-related genes were identified using Gene Set Enrichment Analysis (GSEA) (http://www.gsea-msigdb.org/gsea/index.jsp). Additionally, the gene set M24779.gmt, containing eight necroptosis genes, was retrieved using the keyword "necroptosis", yielding a total of 67 necroptosis-associated genes.

Additionally, to evaluate the link between these differentially expressed necroptosis-related genes, we constructed a PPI network using the interacting gene/protein search engine (String, http://www.string-db.org/); then, we calculated Pearson correlations between genes.

Development and validation of the necroptosis-related gene prognostic mode

To examine the prognostic significance of localized death-associated genes in LGGs, we used One-Way COX regression analysis on the training set to identify DEGs genes that were significantly linked with overall survival (OS). Then, in order to minimize overfitting, we employed the least absolute shrinkage and selection operator (LASSO) penalized Cox proportional risk regression. The procedure described above was carried out using the R package "glmnet" and a minimum criterion to compute the penalty parameter [7]. Additionally, we used Kaplan-Meier survival analysis to clarify the relationship between DEGs genes and overall survival (OS). Kaplan-Meier survival analysis was performed to determine the best possible risk threshold for the TCGA cohort. The glioma patients in the TCGA cohort were divided into low- and high-risk score sub-groups based on the appropriate cutoff value. Patients with primary glioma had their survival predicted using the risk signature, and this accuracy was determined using Kaplan-Meier survival curves and receiver operating characteristic (ROC) curves. Necroptosis risk signature validity was assessed using data from two CGGA cohorts. On the basis of the findings of multifactor Cox regression analysis, prognostic models were created. Patients were classified as high- or low-risk based on the median of their risk scores. The calculation for the risk score was as follows: risk score = n iXi xYi (n: number of surviving genes after lasso regression; X: coefficients; Y: gene expression level). The OS time was compared between the two groups using Kaplan-Meier analysis. At three and five years, ROC analysis was done using the "survivalROC" program, and the area under the curve (AUC) was also computed. The CGGA data set was utilized as a validation set for calculating risk scores and performing Kaplan-Meier and Receiver Operating Characteristic Curve (ROC) analyses.

On the other hand, to determine if the risk signature may be used as a biomarker for assess-

ing glioma patients' prognosis, univariate and multivariate studies were carried out. Afterward, we used stratified analysis to investigate the connection between the risk signature and a number of other types of clinical characteristics. Additionally, we used univariate Cox analysis to determine clinical features of prognostic value and create a nomogram based on the risk score. Calibration and ROC curves were used to assess the nomogram's efficacy at 1, 3, and 5 years.

Functional enrichment analysis

The Gene Ontology (GO) and Kyoto Encyclopedia of Genes and Genomes (KEGG) annotations were conducted using the R package "ClusterProfiler" based on the difference between high and low risk groups (|log2FC|>1; *P* Value 0.05). In addition, analysis of KEGG (Kyoto Encyclopedia of Genes and Genomes) enrichment was also assessed [18].

Estimation of tumor-infiltrating immune cells

Using the cell type identification analysis in the "CIBERSORT" R package [10], we computed the proportional number of immune infiltrating cells in all tumor samples based on the transcriptional profile of LGGs in TCGA. The Wilcoxon rank sum test was performed to compare the immune infiltration levels between high- and low-risk groups.

Statistical analysis all statistical analyses

In this research were done using R program (version 3.6.3). The log-rank test was employed for the Kaplan-Meier survival analysis. Hazard ratios (HRs) and 95% confidence intervals (CIs) were given when appropriate. *P* value less than 0.05 was consider as significant difference.

Result

Identification of DEGs between normal and tumor tissues

We compared 67 necroptosis-related genes in low-grade glioma patients and healthy controls using the GEPIA2 (http://gepia2.cancer-pku.cn) database and identified 21 differentially expressed genes (**Figure 1A**), conditional on (|log2FC|>1; *P* Value 0.05). All 21 genes were up-regulated in this group. In low-grade glioma vs normal tissues, CDKN2A, EGFR, MYC, IDH1, and TNFRSF21 were differently multiplied by >4 (log2FC>2). We did Pearson correlation analysis on these genes and displayed the PPI network to further study their connections (**Figure 1B**). The correlation heat map demonstrated that the majority of gene phases had substantial positive correlations, indicating that gene interactions were rather robust. The genes with the highest frequency of occurrence had a significant positive correlation to the IDH1 gene, followed by those with a high positive correlation to the DIABLO gene. The map of protein interaction networks revealed that the majority of genes interacted with the MYC gene. Three genes, SLC39A7, IPMK, and PANX1, were shown to be unrelated to other genes.

Development of prognostic gene model in the training set and testing set

We screened data from 388 patients to identify differentially expressed genes associated with scorched death using univariate Cox regression analysis (P<0.01). We identified 15 genes (**Figure 2A**, **2B**) through preliminary analysis of differentially expressed genes associated with scorched death using one-way Cox regression analysis (P<0.01). We then screened the characteristic prognostic genes using LASSO regression analysis and Kaplan-Meier survival analysis (P<0.05), and the ten genes identified, SIRT1, SLC39A7, HAT1, MYCN, MYC, IDH1, TNFRSF21, TLR3, FADD, and STAT3, were included in the subsequent multifactor COX regression analysis, and a ten-gene prognostic model was developed. The minimum parameter determined the penalty parameter (**Figure 2C**, **2D**). **Figure 3** showed the KM curves of the potential genes in the TCGA. **Figure 4** also depicts the risk score distribution, patient survival, and expression heat map for the ten prognostic genes. The multifactorial COX analysis of the ten genes revealed that SIRT1, HAT1, and IDH1 had the ability to operate as independent prognostic variables, with SIRT1 (HR1) being beneficial for survival and HAT1 and IDH1 (HR>1) being detrimental for survival. The 388 patients were classified into low- and high-risk groups (**Figure 4A**) using the risk score formula's median score. To assess the prognostic model's sensitivity, time-dependent subject operating characteristic (ROC) curves and Kaplan-Meier curves were shown (**Figure 4C**, **4E**). The findings indicated that the survival curves of the high-risk and low-risk groups dif-

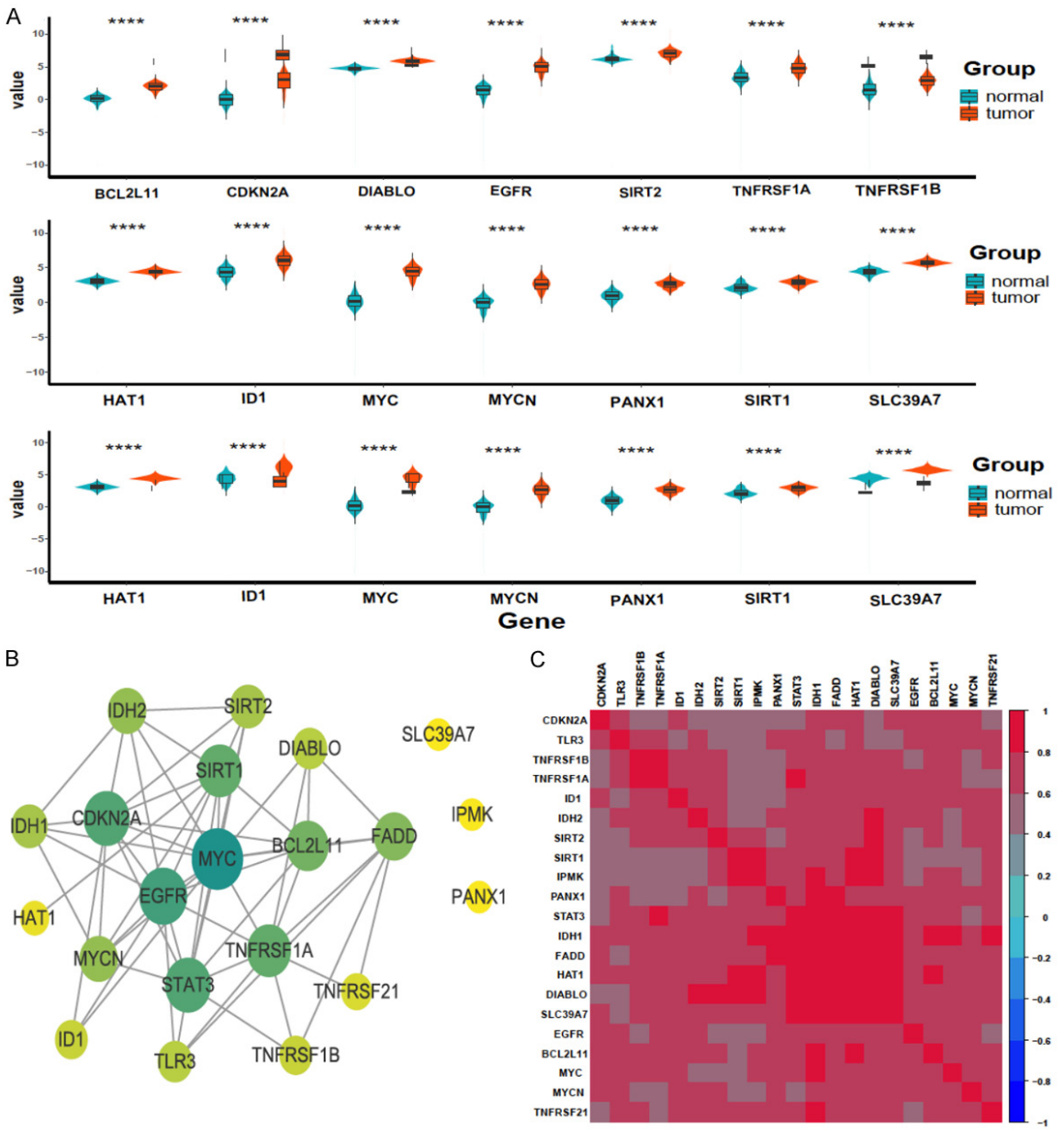

Figure 1. Identification of DEGs between normal and tumor tissues. A. Box plot of between the normal and the tumor tissues (*P<0.1, *P<0.05, **P<0.01, ***P<0.001). B. PPI network showing the interactions of the DEGs (interaction score = 0.9). C. Pearson correlation analysis.

fered significantly (P<0.001). AUC values were 0.842, 0.809, and 0.713 at 1, 3, and 5 years, respectively. Additionally, we used 420 individuals with low-grade glioma from the CGGA database to verify the model (**Figure 4B**, **4D**, **4F**).

Clinical evaluation of the prognostic risk model based on the training set

To test the clinical utility of prognostic evaluation, we investigated the connection between risk scores and clinical variables using univariate and multivariate COX approaches. In the univariate COX analysis, we discovered that patient age, grading, radiation, and risk score were all significantly linked with OS (**Figure 5A**, **5B**, P<0.001). Interestingly, a similar pattern was discovered in multifactor COX. As a result, necrotizing apoptosis is strongly related to the prognosis of low-grade gliomas. Meanwhile, we discovered variations in the age and grade dis-

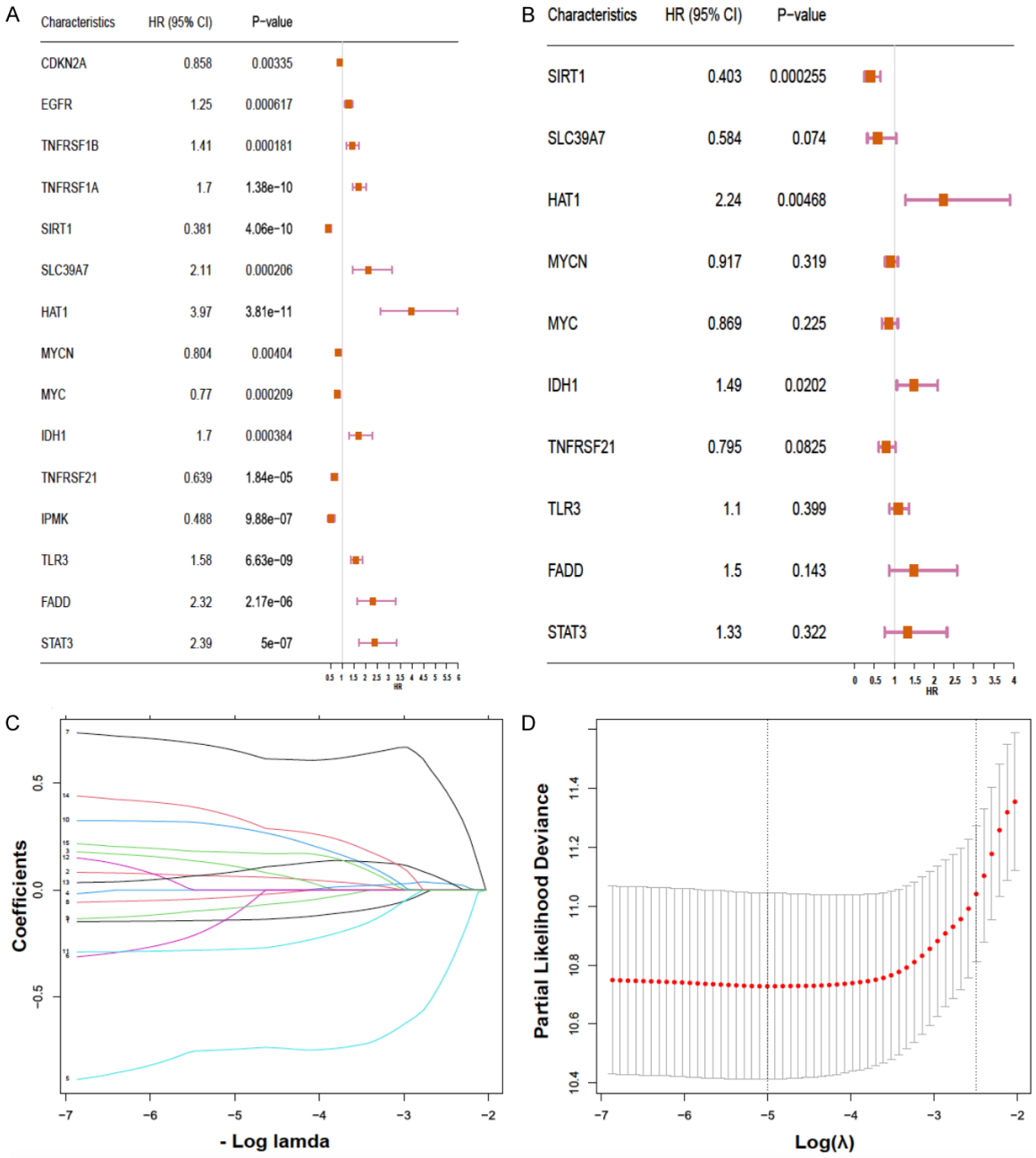

Figure 2. DEGs with univariate Cox regression. Identification of prognostic signatures in the training set. A, B. Univariate COX analysis of DEGs. C. Cross-validation for tuning parameter screening in the LASSO regression model. D. Coefficient profiles in the LASSO regression model.

tributions of patients in the low- and high-risk categories (**Figure 5C**). When combined with the findings of multivariate Cox regression analysis, the risk score may serve as an independent predictor of LGG in the whole group. Meanwhile, when the risk score was paired with additional clinicopathological parameters, the ROC curve indicated that the AUC rose, suggesting that the risk score was an independent predictive factor (**Figure 5D-F**).

Developing and validating a nomogram that incorporates clinical features

In the TCGA cohort, we incorporated clinical information to construct a Nomogram plot. A total score for each patient was calculated by adding the results for each prognostic criterion. Patients with greater overall scores showed worse clinical outcomes (**Figure 6**), with the predicted and actual survival rates agreeing perfectly.

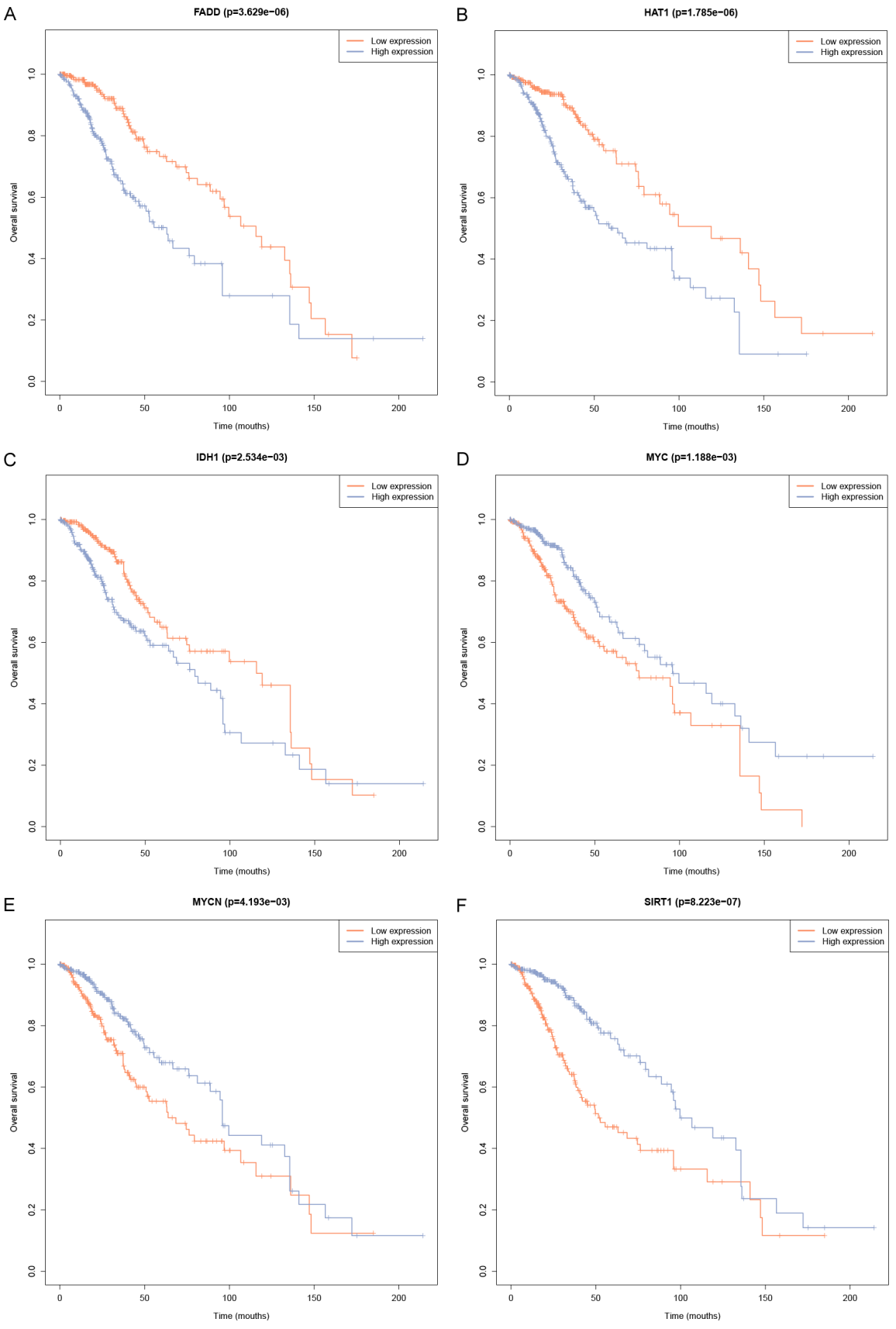
A
FADD (p=3.629e−06)
B
HAT1 (p=1.785e−06)
C
IDH1 (p=2.534e−03)
D
MYC (p=1.188e−03)
E
MYCN (p=4.193e−03)
F
SIRT1 (p=8.223e−07)
Low expression
High expression
Overall survival
Time (mouths)

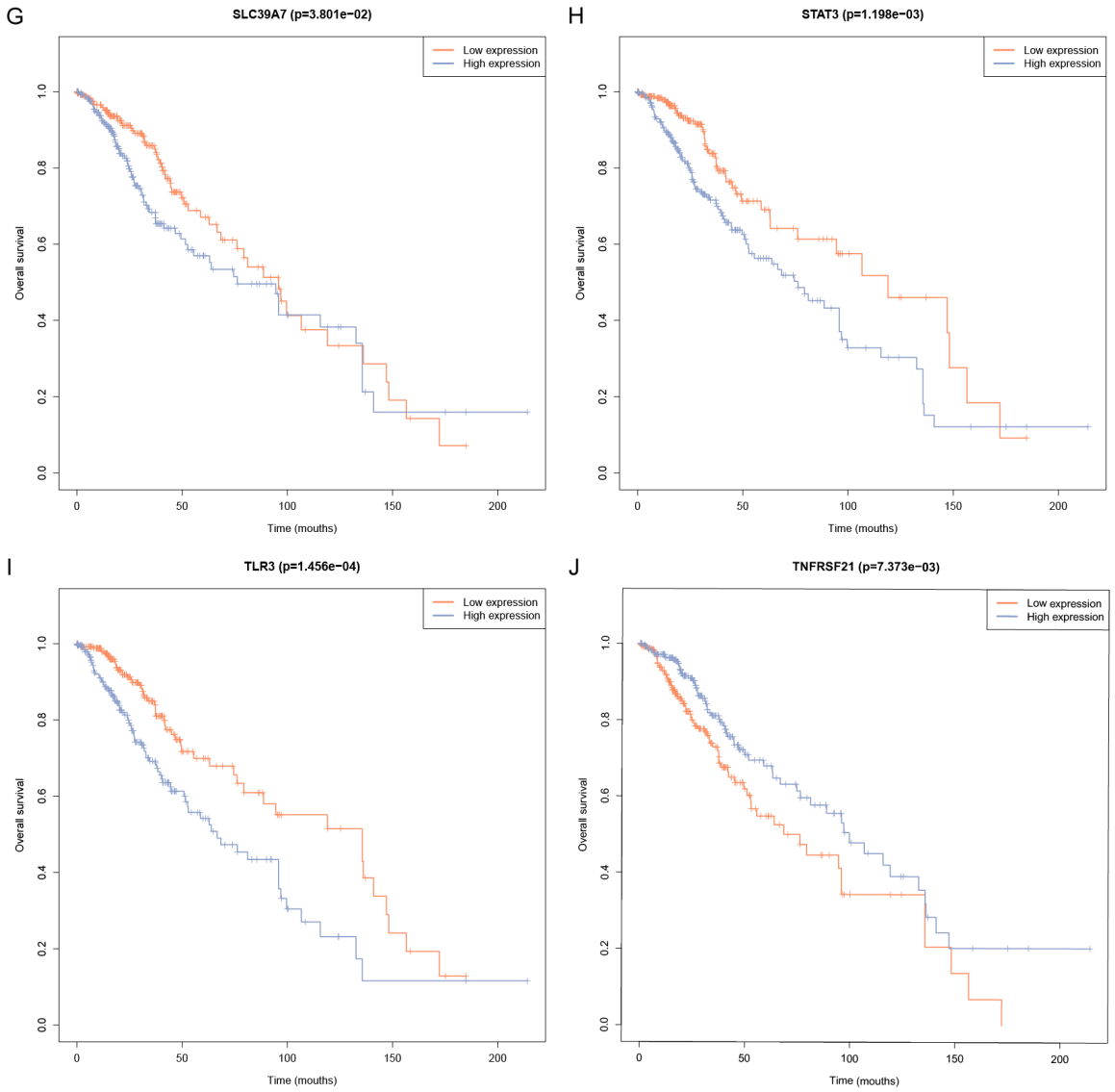

Figure 3. The log-rank test of KM curves of the selected genes in the risk model in TCGA.

Functional analyses based on the risk model

We extracted DEGs using the "limma" R tool to further investigate subgroup-related pathways defined by the risk model. Between the low- and high-risk categories in the TCGA cohort, a total of 28 DEGs were found (**Figure 7A**). There were 19 up-regulated genes and 9 down-regulated genes among them. We conducted GO enrichment and KEGG pathway analyses based on differences between high and low risk groups (**Figure 7B** and **7C**). The most enriched pathways are those associated to iron bioengineering and Alzheimer's disease.

Immune cell infiltration, tumor somatic mutation, and tumor microenviro-nment characteristics of riskscore in TCGA-LGGs cohort

The difference in somatic mutation distribution between the high-risk and low-risk groups (**Figure 8A** and **8B**) was displayed using the R package "maftools". The mutation rates were comparable across the high-risk (48.82%) and low-risk (48.82%) groups (46.06%). The cell stromal cell score, immune cell score, and composite score were calculated using the ESTIMATE method (**Figure 9A** and **9B**), and the relative number of 22 immune cell types in

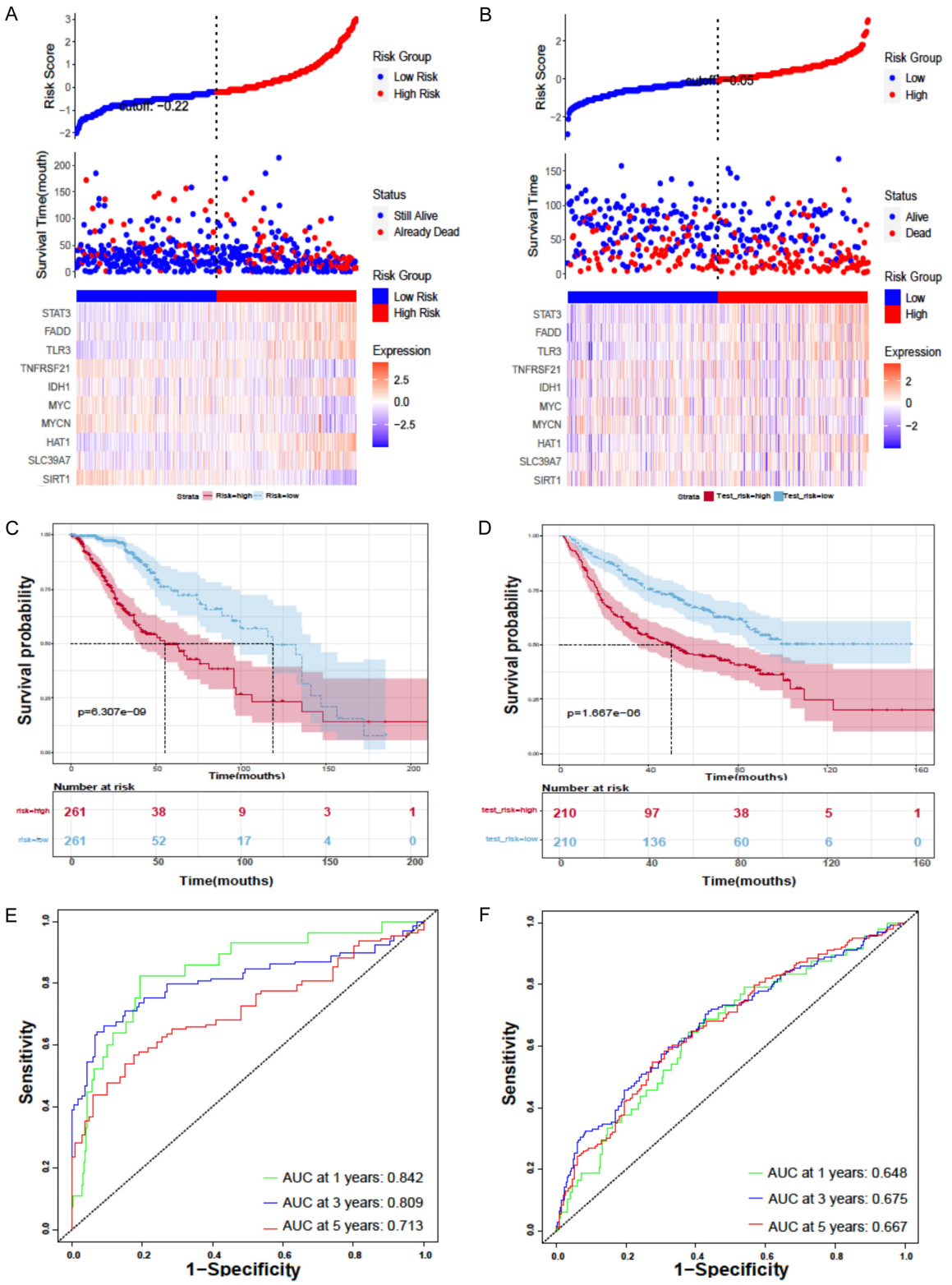

Figure 4. Risk score analysis, survival analysis, and prognostic performance of a risk-score model based on differential expression of iron metabolism-related genes in patients with LGG. Risk score and survival time distributions, and heatmaps of gene-expression levels of the iron-metabolism signature in the TCGA (A) and CGGA (B) cohorts. KM curves of the risk score model for predicting OS in the TCGA (C) and CGGA (D) cohorts. ROC curves and AUC values of the risk score model for predicting the 1-, 3-, and 5-year OS times in the TCGA (E) and CGGA (F) cohorts.

A

Characteristics	HR (95% CI)	P−value
Age	1.06	3.03e−15
gender	1.11	0.549
Grade	3.29	4.19e−10
radiation_therapy	2.28	0.000573
riskScore	1.24	2.65e−28

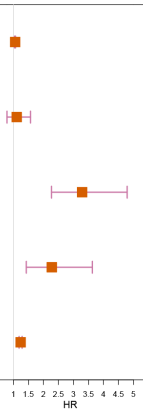

B

Characteristics	HR (95% CI)	P−value
Age	1.04	2.44e−07
gender	1.16	0.443
Grade	2.24	0.000311
radiation_therapy	1.28	0.331
riskScore	1.19	5.33e−14

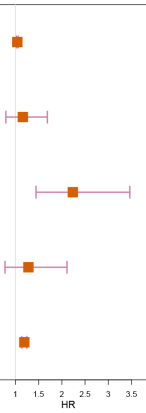

C

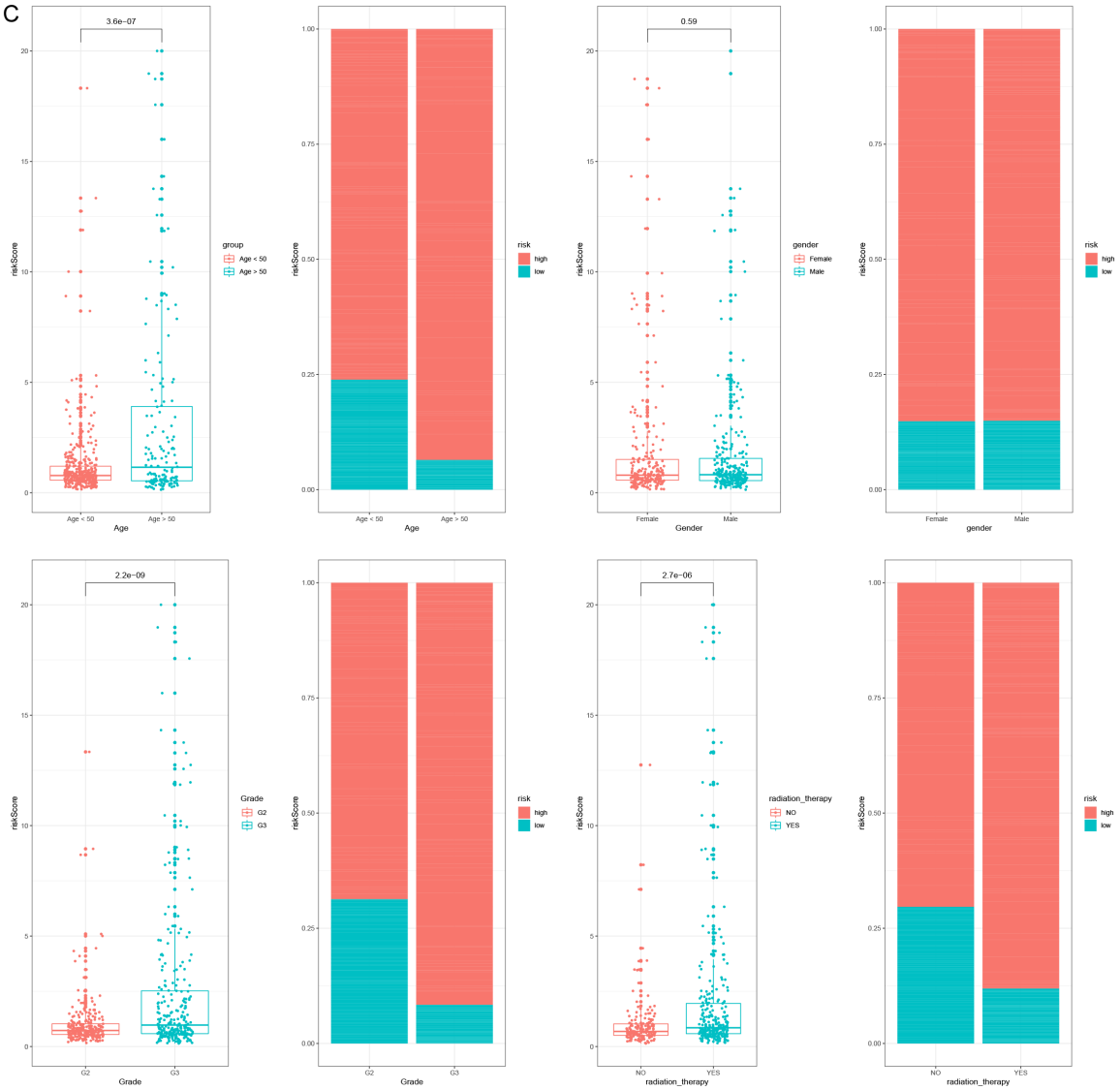

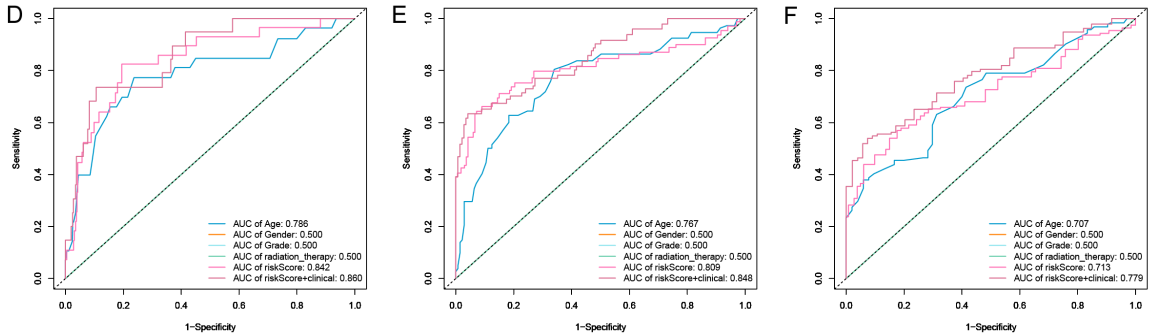

Figure 5. Univariate analysis and Multivariate analysis for hazard ratio values of risk score and clinical characters in the training set. Confidence interval (A and B). (C) The relationship between prognostic gene expression and clinical factors. (D-F) ROC analysis of clinical factors to predict the prognosis of TCGA LGG patients.

each LGGs patient was calculated using the CIBERSORT algorithm. A correlation study of risk ratings and immune cell infiltration revealed that the majority of immune cells were infiltrated considerably differently across the two subtypes (**Figure 9C** and **9D**). Among them, the high-risk group had substantially more activated CD4 memory T cells and M2 type macrophages (P<0.05).

Additionally, to get a better understanding of immune cell features and their link to DEGs, we analyzed the association between immune cell abundance and nine prognostic genes using the TIMER database (**Figure 10**). LGGs were shown to be adversely linked with CD8+ T cells and neutrophils (P = 0.047 and 0.020, respectively). Gls2 expression was inversely connected with CD8+ T cells and neutrophils (P = 0.025 and 0.025, respectively) and positively correlated with B cells (P = 0.013, emC2 [a.k.a. TTC35]) had a negative correlation with B cells, CD4+ T cells, and neutrophils (P<0.001). (P = 0.038, 0.006, and 0.027, respectively).

Discussion

In the current study, three genes were used to develop a prognostic model of necrotizing apoptosis, and all patients were split into high- and low-risk groups. Patients with a high-risk score had a worse overall survival rate (OS) than those with a low-risk score. The area under the curve (AUC) of the receiver operating characteristic (ROC) curve was used to evaluate and confirm this feature's predictive ability. In the TCGA and CGGA cohorts, the nomogram plot showed a high capacity to predict overall survival of LGG patients. GSEA analysis revealed that the high-risk group enriched for inflammatory responses, tumor-related pathways, and pathological processes. Additionally, the high-risk score was associated with invading immune cell expression.

Previous research has revealed necroptosis-associated genes as independent prognostic markers for a number of tumor types. In this work, we examined 21 DEGs linked with necroptosis. After performing Lasso and COX regression analyses, a predictive model comprised of three genes (IDH1, SIRT1, and HAT1) was utilized to categorize LGGs into high-risk and low-risk categories. Subsequent analysis using KM curves, ROC curves, and risk mapping demonstrated that the risk signature performed well in terms of risk groups for the major LGG in the TCGA and CGGA datasets. Additionally, we developed a predictive Nomogram plot model based on genes associated with necroptosis to predict OS in LGG patients. The risk score, as defined by the WHO, was included into the Nomogram plot model. The nomogram plot and receiver operating characteristic analyses demonstrate the line graph's ability to predict OS accurately in the TCGA and CGGA cohorts. The line plot model may be used to assist in determining subsequent treatment of patients.

The IDH2 gene encodes citrate dehydrogenase 2 [19]. Numerous investigations have shown that tumor tissues with changed levels of IDH1 expression and gene alterations [20, 21]. Over 60% of IDH1 gene mutations are found in low-grade gliomas or secondary glioblastomas, as well as in primary glioblastomas [22]. Additionally, IDH mutations may be present early in the illness, since IDH1 mutations have been

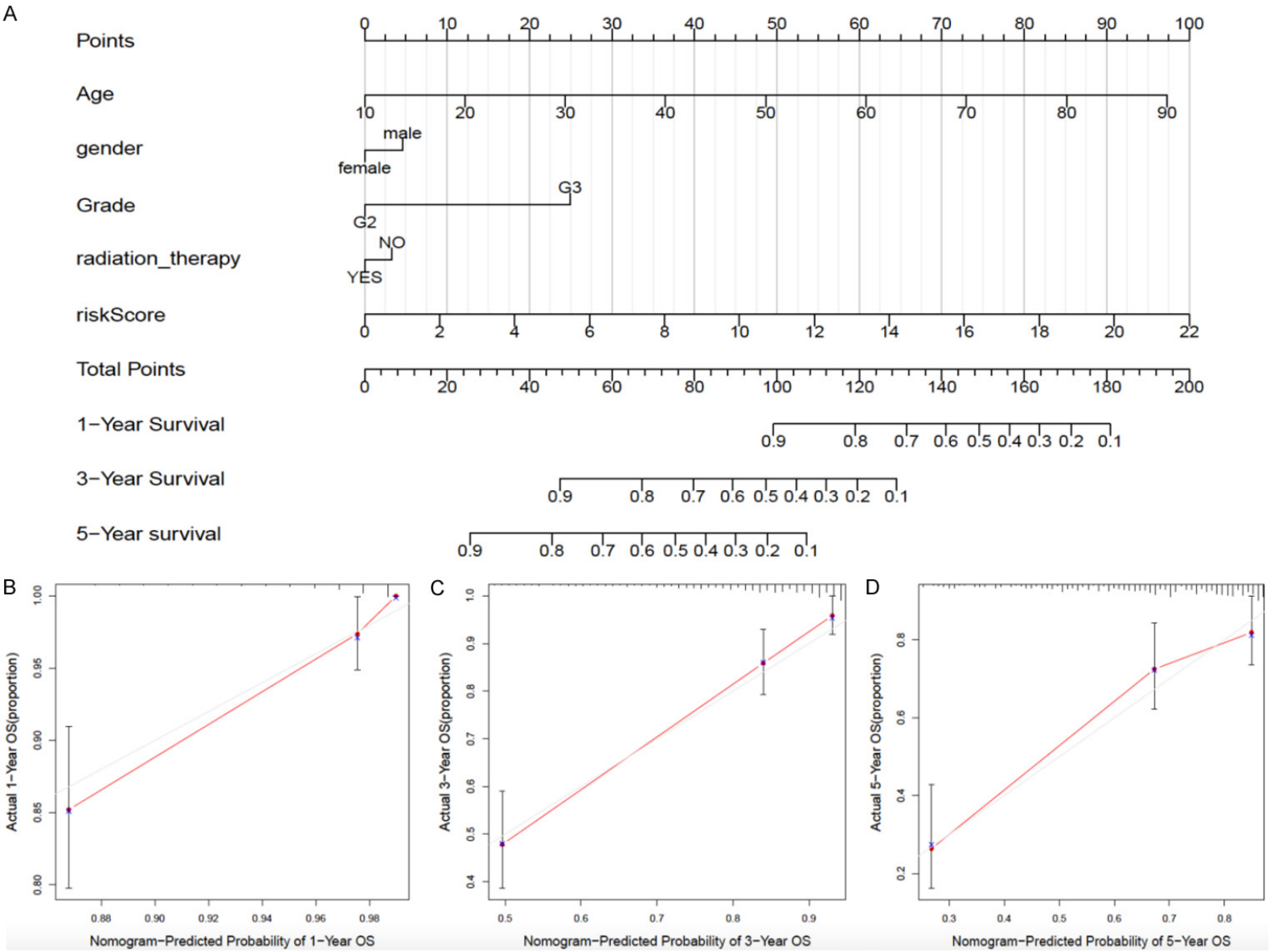

Figure 6. Prognostic nomogram for the 1-, 3-, and 5-year OS times of LGG patients. (A) Independent risk factors screened by multivariate Cox regression in the TCGA cohort were integrated into the nomogram model. (B-D) Calibration curves of the nomogram for predicting 1-, 3-, and 5-year OS in the TCGA.

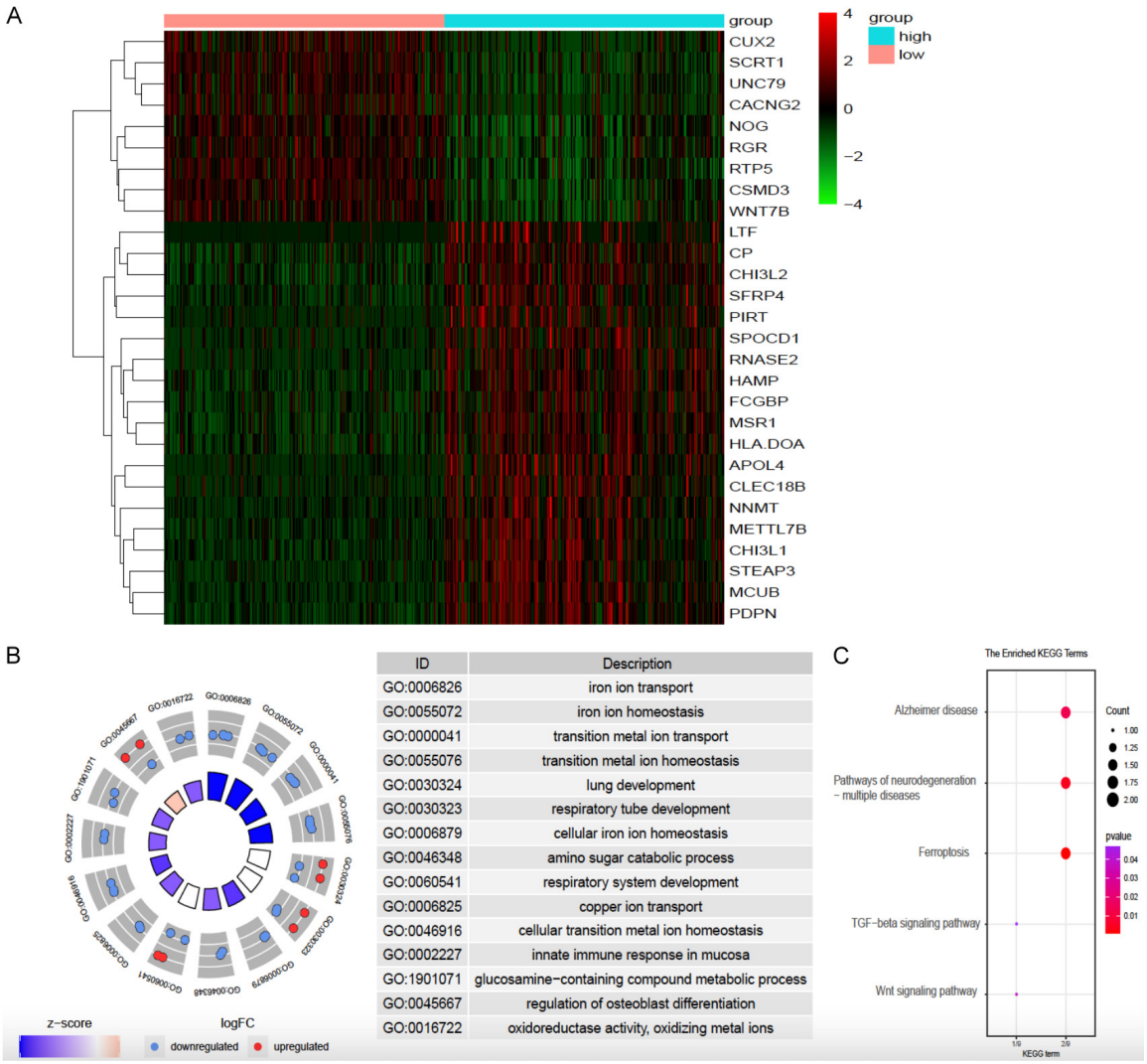

Figure 7. The enriched item in Kyoto Encyclopedia of Genes and Genomes analysis. (A) Different genes Between the low- and high-risk categories in the TCGA cohort. (B) The enriched item in gene ontology analysis. (C) The enriched item in Kyoto Encyclopedia of Genes and Genomes analysis.

reported in some individuals with glioblastoma, which often develops from low-grade gliomas [15]. LGGs are further characterized in the new glioma classification as IDH wild-type or IDH mutant. LGGs are further divided into IDH wild type or mutant type gliomas, which are further classified as oligodendrogliomas with co-deletions of 1p/19q or diffuse astrocytomas with intact 1p/19q patterns but enriched in ATRX and TP53 mutations [23]. Patients with mutated IDH1 had significantly longer survival and progression-free survival than patients with wild-type IDH1 (wild type IDH1) [24]. After correcting for the impact of traditional prognostic variables, IDH1 status was the sole meaningful prognostic factor.

SIRT1 is a sirtuin-family histone deacetylase of class III. Sirtuins have been implicated in a variety of processes including genomic stability, stress responses, and cancer [17-21]. SIRT1 enhances the viability of glioma tumor cell lines and suppresses apoptosis [22]. In addition, Yu et al. showed that SIRT1 may be an initiator of glioma genesis via the PTEN/PI3K/AKT signaling pathway [23]. In comparison, the gene for which we searched, HAT1, has seldom been related to low-grade gliomas in prior research. This presents a novel direction for further research. In conclusion, we created and validated a risk score system for prognosis and risk stratification using necroptosis-associated genes from the TCGA and CGGA datasets. This

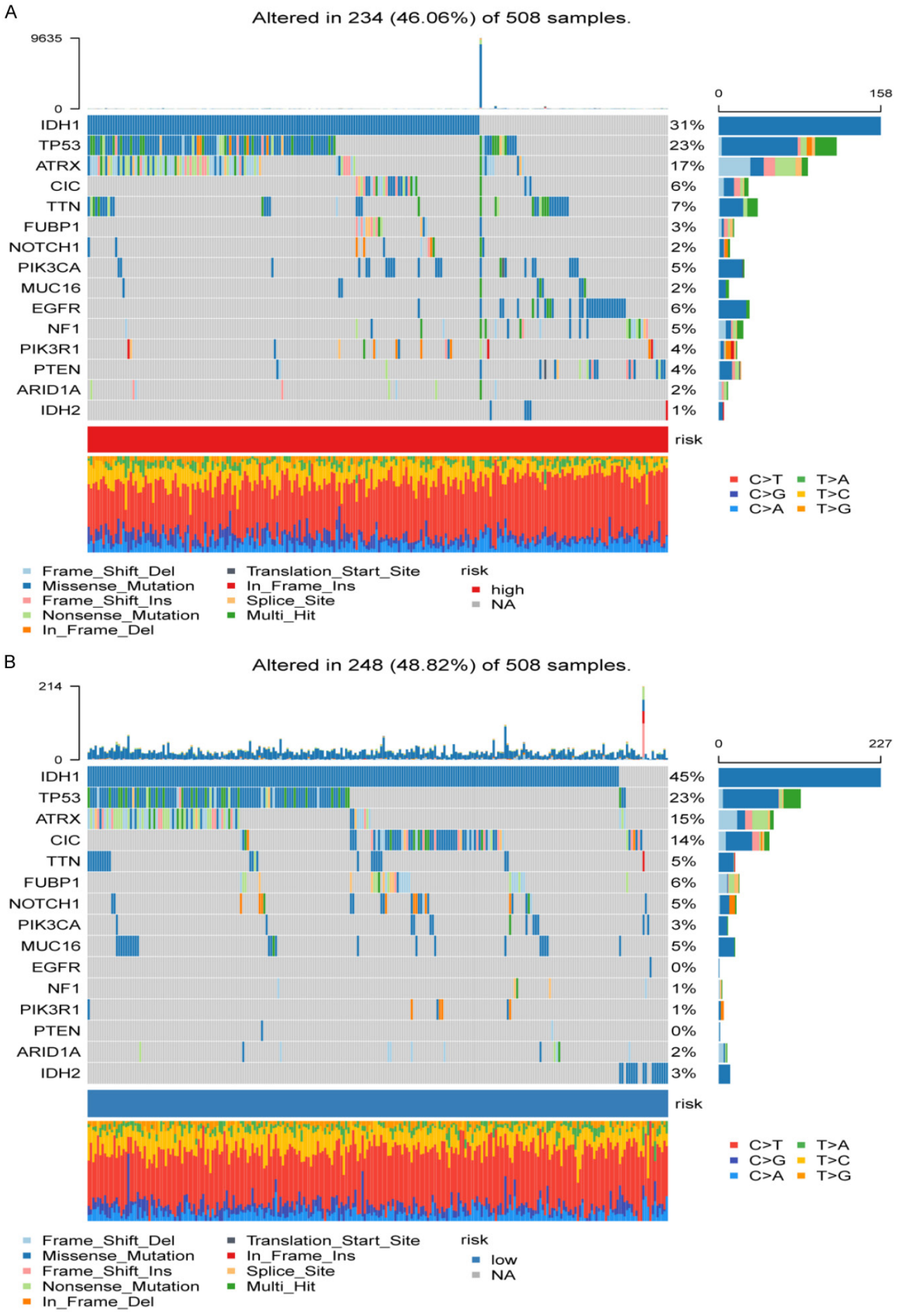

Figure 8. The mutation profile in high- and low-risk groups. A. High-risk group. B. Low-risk group.

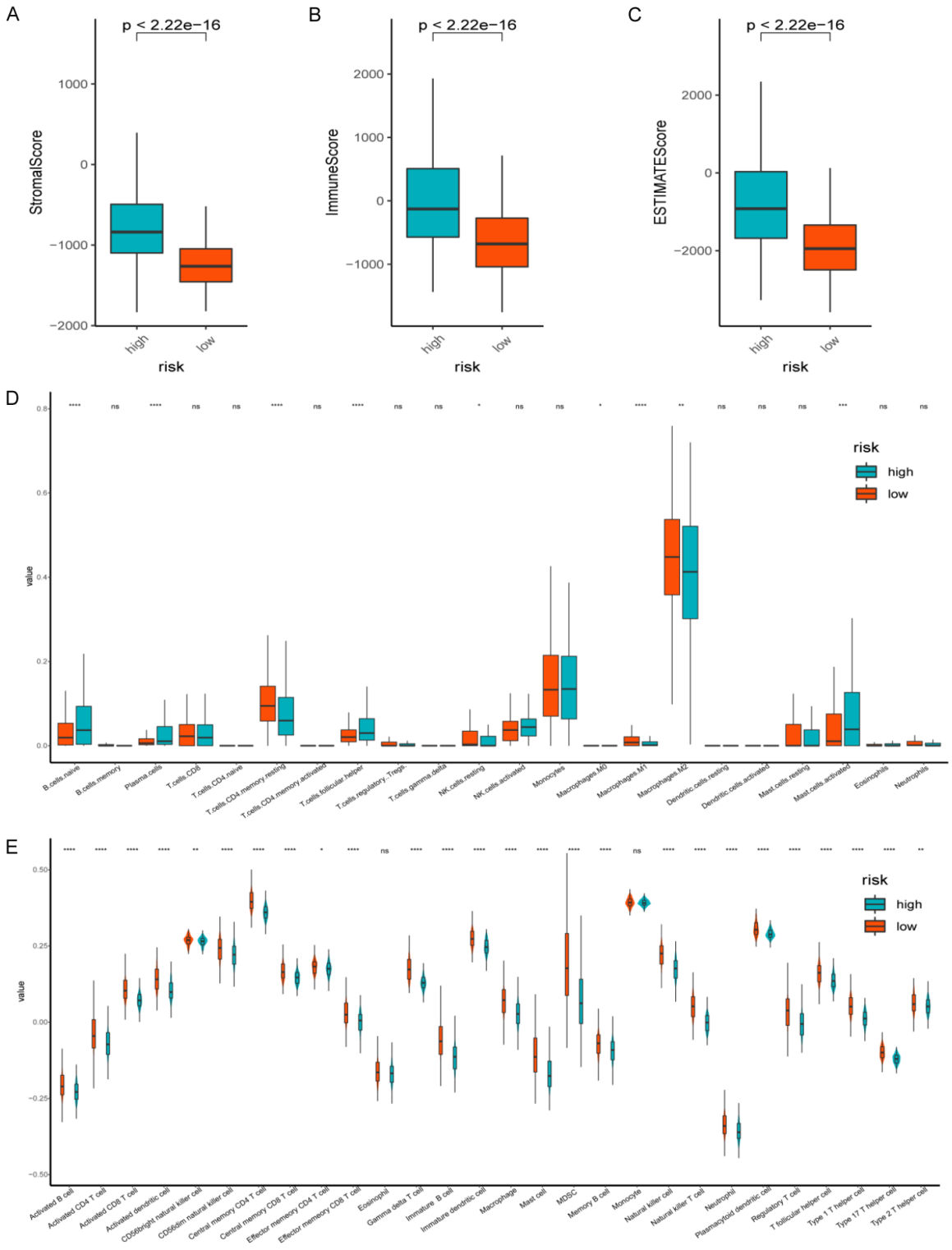

Figure 9. Immune features of risk score. The difference of stromal risk score (A), immune score (B), and estimate score (C). Boxplot indicating the levels of immune cell infiltration in high-risk and low-risk LGG patient (D and E).

prognostic model demonstrated a high degree of predicted accuracy. Our exploratory work offers a theoretical foundation for further investigation into the role of necroptosis genes in glioma. There are still caveats due to the fact that this study was based on the bioinformatics

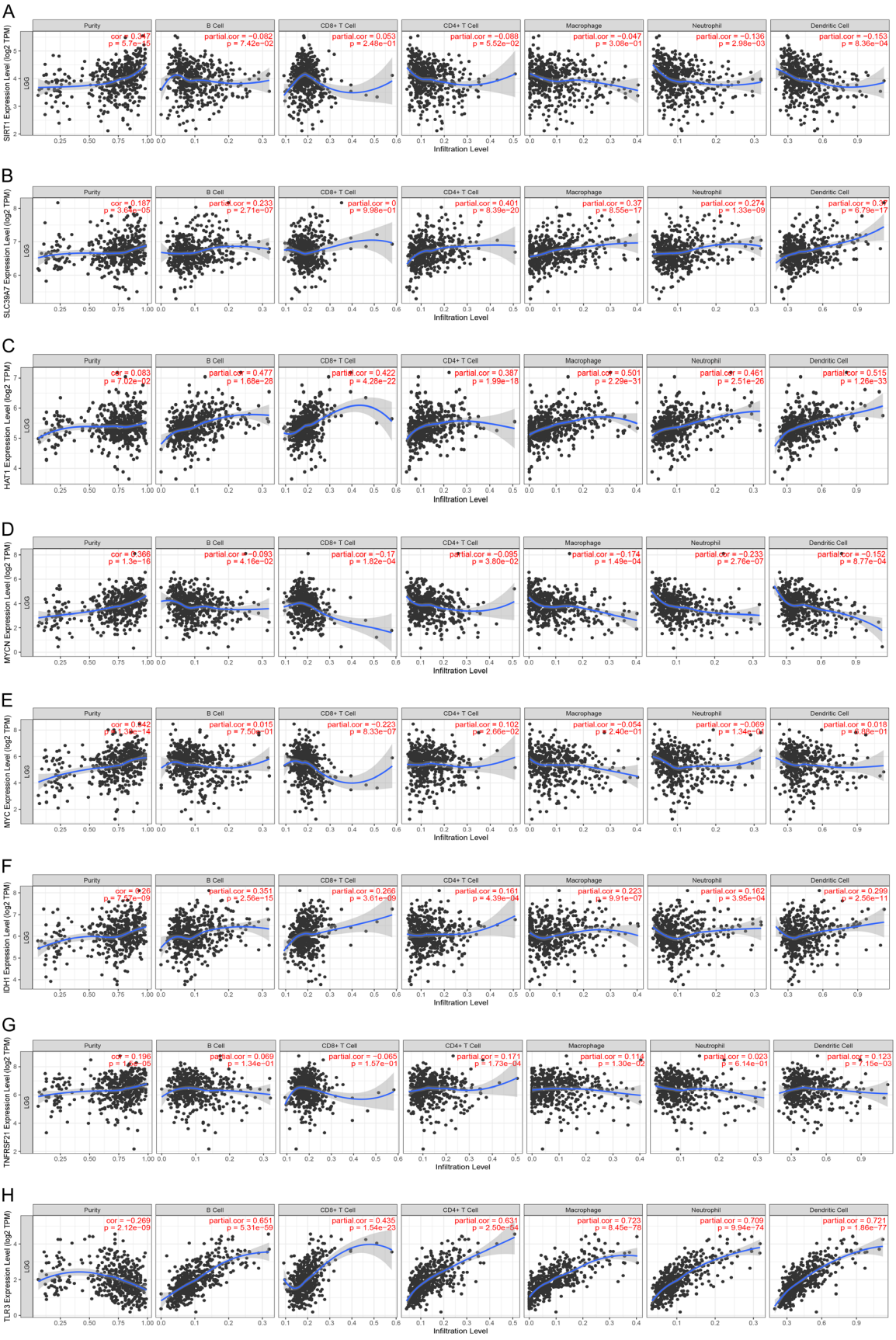
A
SIRT1 Expression Level (log2 TPM)
B
SLC39A7 Expression Level (log2 TPM)
C
HAT1 Expression Level (log2 TPM)
D
MYCN Expression Level (log2 TPM)
E
MYC Expression Level (log2 TPM)
F
IDH1 Expression Level (log2 TPM)
G
TNFRSF21 Expression Level (log2 TPM)
H
TLR3 Expression Level (log2 TPM)
Purity
B Cell
CD8+ T Cell
CD4+ T Cell
Macrophage
Neutrophil
Dendritic Cell
LGG
Infiltration Level

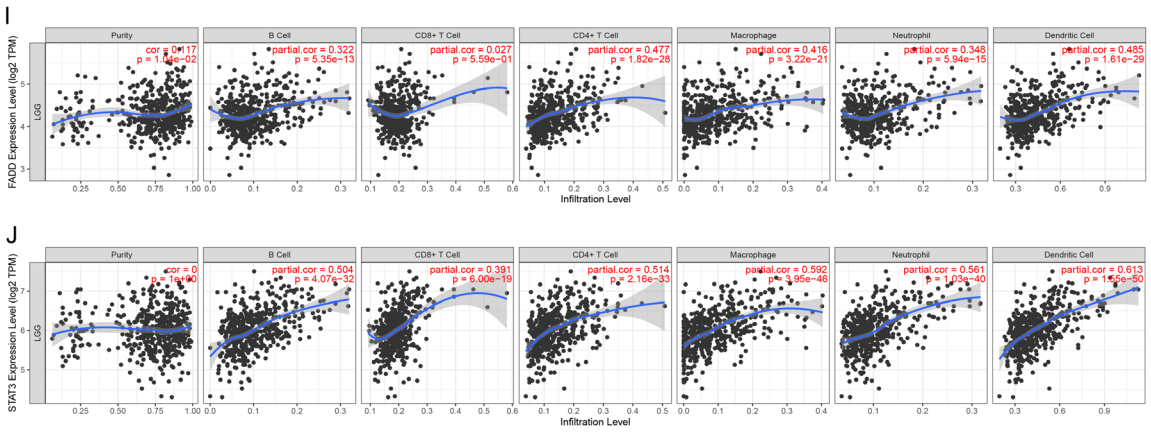

Figure 10. Immune cell infiltration analysis in the TCGA cohort (TIMER).

research. The records were from freely available sources. There is a need for more mechanistic and fundamental experimental research to verify our model and strengthen the foundation of our work, and there is also a need for further research into the clinical prediction capabilities of our model. Finally, necroptosis's significance in gliomas has to be studied in more depth.

Conclusion

Our predictive model based on necroptosis-related genes in LGG was shown to be effective in the diagnosis and prediction of LGG outcome. In addition, we identified possible targets related to necroptosis-related genes for glioma therapy in this study.

Disclosure of conflict of interest

None.

Address correspondence to: Dr. Jue Zhang, Department of Laboratory Medicine, Shuguang Hospital Affiliated to Shanghai University of Traditional Chinese Medicine, Shanghai 201203, China. Tel: +86-021-20256550; E-mail: zhangjue425@hotmail.com

References

[1] Lapointe S, Perry A and Butowski NA. Primary brain tumours in adults. Lancet 2018; 392: 432-446.

[2] Louis DN, Perry A, Reifenberger G, Von Deimling A, Figarella-Branger D, Cavenee WK, Ohgaki H, Wiestler OD, Kleihues P and Ellison DW. The 2016 World Health Organization classification of tumors of the central nervous system: a summary. Acta Neuropathol 2016; 131: 803-820.

[3] Smoll NR, Gautschi OP, Schatlo B, Schaller K and Weber DC. Relative survival of patients with supratentorial low-grade gliomas. Neuro Oncol 2012; 14: 1062-1069.

[4] Stupp R, Taillibert S, Kanner AA, Kesari S, Steinberg DM, Toms SA, Taylor LP, Lieberman F, Silvani A, Fink KL, Barnett GH, Zhu JJ, Henson JW, Engelhard HH, Chen TC, Tran DD, Sroubek J, Tran ND, Hottinger AF, Landolfi J, Desai R, Caroli M, Kew Y, Honnorat J, Idbaih A, Kirson ED, Weinberg U, Palti Y, Hegi ME and Ram Z. Maintenance therapy with tumor-treating fields plus temozolomide vs temozolomide alone for glioblastoma: a randomized clinical trial. JAMA 2015; 314: 2535-2543.

[5] van den Bent MJ, Dubbink HJ, Sanson M, van der Lee-Haarloo CR, Hegi M, Jeuken JW, Ibdaih A, Brandes AA, Taphoorn MJ and Frenay M. MGMT promoter methylation is prognostic but not predictive for outcome to adjuvant PCV chemotherapy in anaplastic oligodendroglial tumors: a report from EORTC brain tumor group study 26951. J Clin Oncol 2009; 27: 5881.

[6] Ludwig K and Kornblum HI. Molecular markers in glioma. J Neurooncol 2017; 134: 505-512.

[7] Molinaro AM, Taylor JW, Wiencke JK and Wrensch MR. Genetic and molecular epidemiology of adult diffuse glioma. Nat Rev Neurol 2019; 15: 405-417.

[8] Krysko O, Aaes TL, Kagan VE, D'Herde K, Bachert C, Leybaert L, Vandenabeele P and Krysko DV. Necroptotic cell death in anti-cancer therapy. Immunol Rev 2017; 280: 207-219.

[9] Robinson N, McComb S, Mulligan R, Dudani R, Krishnan L and Sad S. Type I interferon induces necroptosis in macrophages during infec-

tion with Salmonella enterica serovar Typhimurium. Nat Immunol 2012; 13: 954-962.
[10] Roychowdhury S, McMullen MR, Pisano SG, Liu X and Nagy LE. Absence of receptor interacting protein kinase 3 prevents ethanol-induced liver injury. Hepatology 2013; 57: 1773-1783.
[11] Fan H, Tang HB, Kang J, Shan L, Song H, Zhu K, Wang J, Ju G and Wang YZ. Involvement of endoplasmic reticulum stress in the necroptosis of microglia/macrophages after spinal cord injury. Neuroscience 2015; 311: 362-373.
[12] Zhu F, Zhang W, Yang T and He SD. Complex roles of necroptosis in cancer. J Zhejiang Univ Sci B 2019; 20: 399-413.
[13] Gong Y, Fan Z, Luo G, Yang C, Huang Q, Fan K, Cheng H, Jin K, Ni Q and Yu X. The role of necroptosis in cancer biology and therapy. Mol Cancer 2019; 18: 100.
[14] Bozec D, Iuga AC, Roda G, Dahan S and Yeretssian G. Critical function of the necroptosis adaptor RIPK3 in protecting from intestinal tumorigenesis. Oncotarget 2016; 7: 46384.
[15] Seifert L, Werba G, Tiwari S, Giao Ly NN, Alothman S, Alqunaibit D, Avanzi A, Barilla R, Daley D and Greco SH. The necrosome promotes pancreatic oncogenesis via CXCL1 and Mincle-induced immune suppression. Nature 2016; 532: 245-249.
[16] Grootjans S, Vanden Berghe T and Vandenabeele P. Initiation and execution mechanisms of necroptosis: an overview. Cell Death Differ 2017; 24: 1184-1195.
[17] Jiang X, Shi Y, Chen X, Xu H, Liu B, Zhou F, Huang X, Cho WC, Li L and Pu J. NCAPG as a novel prognostic biomarker in glioma. Front Oncol 2022; 12: 831438.
[18] Liu J, Lan Y, Tian G and Yang J. A systematic framework for identifying prognostic genes in the tumor microenvironment of colon cancer. Front Oncol 2022; 12: 899156.
[19] Dimitrov L, Hong CS, Yang C, Zhuang Z and Heiss JD. New developments in the pathogenesis and therapeutic targeting of the IDH1 mutation in glioma. Int J Med Sci 2015; 12: 201-213.
[20] Robbins D, Wittwer JA, Codarin S, Circu ML, Aw TY, Huang TT, Van Remmen H, Richardson A, Wang DB, Witt SN, Klein RL and Zhao Y. Isocitrate dehydrogenase 1 is downregulated during early skin tumorigenesis which can be inhibited by overexpression of manganese superoxide dismutase. Cancer Sci 2012; 103: 1429-1433.
[21] Li W and Zhao Y. Withaferin A suppresses tumor promoter 12-O-tetradecanoylphorbol 13-acetate-induced decreases in isocitrate dehydrogenase 1 activity and mitochondrial function in skin epidermal JB6 cells. Cancer Sci 2013; 104: 143-148.
[22] Wesseling P and Capper D. WHO 2016 classification of gliomas. Neuropathol Appl Neurobiol 2018; 44: 139-150.
[23] Louis DN, Perry A, Reifenberger G, von Deimling A, Figarella-Branger D, Cavenee WK, Ohgaki H, Wiestler OD, Kleihues P and Ellison DW. The 2016 world health organization classification of tumors of the central nervous system: a summary. Acta Neuropathol 2016; 131: 803-820.
[24] Dahlrot RH, Kristensen BW, Hjelmborg J, Herrstedt J and Hansen S. A population-based study of low-grade gliomas and mutated isocitrate dehydrogenase 1 (IDH1). J Neurooncol 2013; 114: 309-317.